Secreted frizzled related-protein 2 is prognostic for human pancreatic cancer patient survival and is associated with fibrosis

Julie B. Siegel[a], Patrick Nasarre[a], Lillian Hsu[a], Rupak Mukherjee[a], Meghan Gormley[a],
Bailey Richardson[a], Imran Khan[b,c], Jordan E. Morningstar[d], Eleanor Hilliard[a], John P. O'Bryan[b,c],
Kristi L. Helke[e], Laura Spruill[f], Nathan G. Dolloff[b] and Nancy Klauber-DeMore[a]
[a]*Department of Surgery, Hollings Cancer Center, Medical University of South Carolina, Charleston, SC, USA*
[b]*Department of Cellular and Molecular Pharmacology and Experimental Therapeutics, Hollings Cancer Center,
Medical University of South Carolina, Charleston, SC, USA*
[c]*Ralph H. Johnson VA Medical Center, Charleston, SC, USA*
[d]*Department of Regenerative Medicine and Cell Biology, Medical University of South Carolina, Charleston SC, USA*
[e]*Department of Comparative Medicine, Medical University of South Carolina, Charleston, SC, USA*
[f]*Department of Pathology and Laboratory Medicine, Medical University of South Carolina, Charleston, SC, USA*

Abstract. Pancreatic adenocarcinoma (PDAC) is one of the deadliest cancers, with five-year survival rates of 9%. We hypothesized that secreted frizzled-related protein 2 (SFRP2) may influence stromal growth in pancreatic cancer, since it increases fibrosis and collagen production in non-neoplastic pathologies. We assessed SFRP2 value as a biomarker and assessed its function in PDAC. *SFRP2* gene expression in patients with PDAC was analyzed using TCGA data. Disease free survival (DFS) was analyzed using Kaplan Meier test. The effect of KRAS inhibition on SFRP2 expression in PDAC cells was assessed. The associations of stromal content with SFPR2 mRNA and protein with fibrosis were analyzed. The role of SFRP2 in mesenchymal transformation was assessed by western blot in fibroblasts. Of all cancers in TCGA, SFRP2 levels were highest in PDAC, and higher in PDAC than normal tissues ($n = 234$, $p = 0.0003$). High *SFRP2* levels correlated with decreased DFS ($p = 0.0097$). KRAS inhibition reduced SFRP2 levels. Spearman correlation was 0.81 between stromal RNA and SFRP2 in human PDAC, and 0.75 between fibrosis and SFRP2 levels in PDAC tumors. SFRP2-treated fibroblasts displayed mesenchymal characteristics. *SFRP2* is prognostic for PDAC survival, regulated by KRAS, and associated with PDAC fibrosis.

Keywords: SFRP2, pancreas, fibroblast, cancer biomarkers, KRAS

1. Introduction

Pancreatic adenocarcinoma (PDAC) is the fourth leading cause of cancer deaths in the United States [1], and *KRAS* is mutated in 90% of patients with PDAC [2].

Even with improved chemotherapy regimens, the 9% five-year survival remains low [3]. One of the barriers to pancreatic cancer treatment is its desmoplastic stroma. Pancreatic cancer has the highest level of stroma ($\sim$ 80% of its mass) of any solid organ tumor [4], which decreases the tumor vasculature and raises the interstitial pressure, shielding the tumor from chemotherapy and immune response [5]. In addition, pancreatic stellate cells are considered the main driver of the desmoplastic reaction, promoting cancer progression [6].

*Corresponding author: Nancy Klauber-DeMore, BMW Endowed Chair Cancer Research, Medical University of South Carolina, MSC 295, Room 240, 114 Doughty Street, Charleston, SC 29425, USA. Tel.: +1 843 876 0179; E-mail: demore@musc.edu.

Secreted frizzled-related protein 2 (SFRP2) is a glycoprotein upregulated in multiple cancer types that contributes to tumor growth, migration, anti-apoptosis [7–14], and angiogenesis [7,9,13]. SFRP2 upregulates markers of immune dysfunction (PD-1 and CD38) in T-cells and contributes to their exhaustion [15]. We previously developed a humanized monoclonal antibody to SFRP2 (hSFRP2 mAb) that inhibits tumor growth, angiogenesis, induces tumor apoptosis [15,16], and overcomes resistance to PD-1 inhibition [15]. We hypothesized that SFRP2 may influence stromal growth in cancer, since it increases fibrosis in non-neoplastic pathologies [17,18]. A high correlation between SFRP2 mRNA expression and stromal mRNA expression in bladder, breast, colorectal, glioblastoma, head and neck, kidney, lung, ovarian, and endometrial cancers has also been found [19]. In correlation network analyses, genes involved in EMT process and ECM structure were associated with *SFRP2* expression [19]. Because of the high stromal content in pancreatic cancer, we hypothesized that SFRP2 may play a larger role in this tumor type, not only through reducing apoptosis, increasing angiogenesis, and affecting immune cell activation, but also through activation of fibroblasts in the tumor stroma and development of a myofibroblast phenotype.

We sought to explore the relationship between SFRP2 and pancreatic cancer to determine whether *SFRP2* expression is associated with survival and tumor fibrosis, and whether it is regulated by KRAS, a major driver of PDAC. Additionally, we investigated the ability of SFRP2 to promote the mesenchymal transformation of fibroblasts and stimulation of fibrinogen production.

2. Methods

2.1. Cell lines, cell isolation, and tissue culture

Pancreatic cancer cell lines AsPC-1, MIA PaCa-2, and Panc02-luc were donated by Dr. Ernest Ramsay Camp (Medical University of South Carolina). Panc02-luc were originally obtained from the NCI DCTD Tumor Repository and transfected as previously described [20]; AsPC-1 and MIA PaCA-2 were from American Type Culture Collection (ATCC CRL-1420). PANC-1[R15] and PSN-1[R15] cells were generated as previously described [21]. Primary human skin fibroblasts [22] were donated by Dr. Carol Feghali-Bostwick (Medical University of South Carolina). The mouse angiosarcoma cell line, SVR [23], was purchased from ATCC (#CRL-2280).

A male C57/BL6NCrl mouse purchased from Charles River Laboratory (Wilmington, MA) was used to isolate pancreatic fibroblasts. The pancreas was resected after euthanasia and was washed with ice-cold modified Krebs-Hensleit buffer supplemented with 2.1 g/L sodium bicarbonate (pH 7.4). Next, 1 mL of ice-cold digestion mix (34.4 mL Hanks buffered saline solution (HBSS; #55037C-1000 mL, Sigma-Aldrich, St. Louis, MO, USA), 1 mL Liberase mix (5 mg in 2 mL of HBSS; # 541020001, Roche, Basel, Switzerland), 200 mL 0.25% Trypsin (# 25-050-CL, Corning, Corning, NY, USA), 360 mL 1M HEPES buffer (#H4034-25G, Sigma-Aldrich) was added, and tissue was macerated using a razor blade. The macerated tissue and digestion mix was placed into a 15 mL falcon tube, and an additional 3 mL of digestion mix at 37°C was added. The mix was incubated on a tube rotator at 37°C for 8 min. 10 mL of modified Krebs-Hensleit buffer containing 2.1 g/L sodium bicarbonate (#K3753, Sigma-Aldrich) was added to quench the digestion, and the mixture was briefly rested to allow the tissue chunks to collect at the bottom. The supernatant containing the cellular suspension was removed and placed on ice. Digestion mix (3 mL at 37°C) was added and another round of incubation on the tube rotator was performed for 8 min. Once again, the supernatant was placed on ice, and the digestion was repeated until no visible chunks of tissue remained in the tube. The supernatants were then combined in a 50 mL falcon tube, centrifuged for 5 min at 1200 rpm, and washed with 10 mL Krebs-Hensleit buffer and centrifuged again at 1200 rpm for 5 min. Each pellet was finally resuspended in Human Cardiac Fibroblast growth media (#316-500, Cell Applications, San Diego, CA, USA) containing 1% penicillin/streptomycin (#15140122, Thermofisher, Waltham, MA, USA), placed into a 10 cm Petri dish, and grown to confluence.

SVR angiosarcoma, pancreatic cancer MIA PaCA-2 cell line, human skin fibroblasts, and mouse pancreatic fibroblasts were cultured in Dulbecco's Modified Eagle Medium (DMEM, #10-013-CV, Corning) with 10% fetal bovine serum (FBS) (#BT 201-500-D, BioFluid, Fleming Island, FL, USA). AsPC-1 and Panc02-luc pancreatic cancer cell lines were cultured in Roswell Park Memorial Institute (RPMI) media with 10% FBS. All cell lines were cultured at 37°C, 5% CO_2, and 95% humidity.

2.2. In vivo pancreatic cancer GEMM mouse model

Mice experiment protocols were in accordance with the National Institutes of Health guidelines for the

care and use of laboratory animals and approved by the Animal Care and Use Committee (IACUC) at the Medical University of South Carolina. KPC male and female mice (Kras^{tm4Tyj}Trp53^{tm1Brn}Tg(Pdx1-cre/Esr1*)#Dam/J) ($n = 8$) were obtained at 4–8 weeks of age from Jackson Laboratories (Bar Harbor, ME, USA). The sex distribution of more females than males was based on the availability of mice from the vendor. KPC mice are a genetically engineered mouse model (GEMM) with conditionally silenced p53 and *KRAS* mutations that are activated by a Cre recombinase enzyme bound to a mutant estrogen receptor ligand binding domain. Tamoxifen induces Cre recombinase expression, which results in the development of pancreatic intraepithelial neoplasia and eventually PDAC with 100% penetrance [24]. Since animals were provided based on availability, there were seven females and one male. Mice were only housed together if they were littermates. At eight-weeks of age, mice received 100 μL IP injections of tamoxifen 100 mg/kg (#T5648, Sigma-Aldrich) resuspended in corn oil. Pancreatic tumors were resected at end point (age range 4–9 months). Tumors were fixed in formalin and embedded in paraffin. Mice were never fasted and received Harlan Teklad Irradiated 2918 diet, standard water, and were housed in vent-rack caging.

2.3. Antibodies and proteins

Primary antibodies used included rabbit anti-actin (#A2103, Sigma-Aldrich), mouse anti-fibronectin (#610077, BD Biosciences, Franklin Lakes, NJ, USA), rabbit anti-frizzled-5 (H00007855-PW1, Abnova, Taipei, Taiwan), rabbit anti-GAPDH (glyceraldehyde-3-phosphate dehydrogenase, #ab9485, Abcam, Cambridge, MA, USA), rabbit anti-N-cadherin (#ab1221, Abcam), mouse anti-Vinculin (SC #73614, Santa Cruz Biotechnology, Dallas, TX, USA). Rabbit anti-Vinculin (E1E9V) (#13901, Cell Signaling Technologies, Danvers, Massachusetts, USA), Phospho-p44/42 MAPK (Erk1/2) (Thr202/Tyr204) Antibody (#9101, Cell Signaling Technologies, Danvers, Massachusetts, USA), p44/42 MAPK (Erk1/2) Antibody (#9102, Cell Signaling Technologies, Danvers, Massachusetts, USA). Rabbit anti-SFRP2 (#ab86379, Abcam), rabbit anti-SFRP2 (#ab137560 Abcam), and rabbit anti-SFRP2 (#LS-C61791, Lifespan Biosciences, Seattle, Washington, USA) were purchased based on manufacturers' availability. Secondary antibodies used were biotinylated-conjugated anti-rabbit (#BA-1000, Vector Laboratories, Burlingame, CA, USA), horse-radish peroxidase

(HRP)-conjugated anti-mouse (#7076, Cell Signaling, Danvers, MA, USA), HRP-conjugated anti-rabbit (#403005, Southern Biotech, Birmingham, AL, USA), and Goat Anti-Rabbit IgG-HRP (#4030-50, Southern Biotech, Birmingham, AL, USA). Recombinant human SFRP2 protein (SFRP2) was prepared as previously described [25], and provided by the Protein Expression and Purification Core facility from the University of North Carolina, Chapel Hill.

2.4. SFRP2 mRNA expression

SFRP2 mRNA expression levels were determined using the Cancer Genome Atlas (TCGA) database that was accessed on cBioPortal [26,27]. On cBioPortal, the *SFRP2* gene was queried for all cancer types in the TCGA database. *SFRP2* mRNA expression levels were collected for each patient and each cancer type, and descriptive statistics were performed. Gene Expression Profiling Interactive Analysis (GEPIA) [28] is an online tool that includes RNA sequencing data from several databases and can be used for interactive analysis of differential gene expression, profile plotting, survival analysis, and correlation analysis. GEPIA was used to analyze the differential RNA expression of *SFRP2* in pancreatic cancer in the TCGA compared to normal pancreatic tissue. Survival analysis with the Kaplan-Meier method was also conducted through GEPIA to determine the association of disease-free survival with high or low RNA expression of *SFRP2* in TCGA samples. We looked at publicly available datasets to explore percentiles at which there was a statistically significant decrement in survival. Based on these mRNA data, the cutoffs that we can use 20the percentile or less for low group and 50th percentile or greater for the high group provided a statistical separation of survival.

2.5. SFRP2 mRNA expression correlation to stroma in pancreatic cancer

The level of *SFRP2* mRNA expression in pancreatic cancer was obtained in units of fragments per kilobase of transcript per million (FPKM) from the Human Protein Atlas (https://www.proteinatlas.org/about/download) [29]. The level of stromal content for each of these samples was evaluated with the Estimation of Stromal and Immune cells in Malignant Tumor tissues using Expression data (ESTIMATE) provided by the MD Anderson Cancer Center [30]. This scoring uses the TCGA mRNA data to analyze the stromal cell presence in the tumor and the immune cell infiltration. The stro-

mal score was obtained using ESTIMATE, which measures the level of stroma in tumor tissue, and a Spearman correlation between the stromal score and SFRP2 mRNA expression levels for these patient samples was conducted.

2.6. Protein extraction from pancreatic tumor tissues

Human pancreatic tumor samples and their matched normal adjacent tissues from pancreatic resections were obtained from the Medical University of South Carolina Tissue Biorepository. These de-identified tissues were obtained from institutional surgical specimens under an IRB-approved protocol and were stored at $-80°C$ prior to use. Samples were crushed in liquid nitrogen into a fine powder, and 30–100 mg were mixed in Radioimmunoprecipitation assay, or RIPA, buffer (#R3792; TEKnova, Hollister, CA, USA), for protein lysis. Lysates were sonicated, centrifuged at 13,000 g, and supernatants were collected. Lysates were dialyzed, and then additional RIPA buffer was added.

2.7. Immunohistochemistry

Pancreatic tumors were resected from KPC mice, fixed in formalin, paraffin-embedded, and 8 μm thick slices were sectioned. Slides were deparaffinized, rehydrated, and antigen retrieval was performed using heat-mediated, citrate-based Antigen Unmasking Solution (#3300-250, Vector Laboratories) for 30 min. Endogenous peroxidases were blocked with hydrogen peroxide at a concentration of 1:100 (#5155-01, J.T. Baker, Phillipsburg, NJ, USA). Normal goat serum (#50062Z, Thermofisher) was used for non-specific protein blocking. Slides were incubated with the primary antibody (anti-SFRP2 #LS-C61791, Lifespan Biosciences, 1:50), and a negative control was performed with no primary antibody for 90 min at room temperature (RT). Slides were subsequently incubated with the secondary antibody (biotinylated anti-rabbit, 1:150) for 30 min at RT, followed by a 30 min incubation with Vectastain (PK-4000, Vector Laboratories), and an incubation with DAB (#1856090, Thermofisher) followed by a hematoxylin counterstaining (#H3401, Vector Laboratories). Masson Trichrome staining was performed with the Masson Trichrome Staining kit (#84000-286, VWR International, Radnor, PA, USA). Slides were incubated in Bouin solution for 1 hour at 56°C. Slides were consecutively stained with fresh Weigert's hematoxylin for 10 min, Biebrich Scarlet – Acid Fuchsin Solution for 5 min, and then incubated in phosphmolybdic-

phosphotungstic acid solution for 10 min. Tissues were then stained with Aniline Blue solution for 5 min, differentiated in acetic acid solution for 1 minute, dehydrated, and cleared with xylene. Picrosirius red staining was performed by incubating slides for 1 hour in picrosirius red solution containing picric acid (#101410-760, VWR International) and Sirius Red F3B (#43665, Sigma-Aldrich). Slides were washed with two changes of acetic acid solution, then dehydrated and cleared. The pancreatic tumors were ranked by their degree of fibrosis after interpretation of the Masson trichome staining and picrosirius red staining by a veterinarian pathologist (K.L.H.). The SFRP2 staining intensity in tumor cells and percentage of positive tumor cells were scored by a pathologist (L.S.). Each tumor was then ranked by level of SFRP2 staining. These rankings for fibrosis and SFRP2 staining were used to calculate the Spearman correlation coefficient.

2.8. Evaluation of epithelial mesenchymal transformation in fibroblasts

Mouse pancreatic fibroblasts and human skin fibroblasts were plated at 60% confluence in DMEM with 10% FBS and treated with either TGFβ at 5 nM, SFRP2 recombinant protein (SFRP2) at 30 nM, or no treatment. At 48 hours, fibroblasts were removed from the plate, washed twice with PBS, and centrifuged at 500 g for 5 min. Fibroblasts were lysed with RIPA buffer, kept on ice for 15 min, and sonicated.

2.9. Effect of KRAS inhibition on SFRP2 expression in PDAC cells

PANC-1^{R15} and PSN-1^{R15} were treated with doxycycline (DOX) to induce expression of R15 Monobody, which selectively inhibits a subset of oncogenic KRAS proteins including KRAS^{G12D} and KRAS^{G12R} [21]. Following DOX treatment (1–2 μg/mL for 2 days), cells were lysed and then examined for SFRP2 expression by western blot analysis. Previous results confirmed inhibition of the ERK-MAPK pathway in these cells [21]. Additionally, lysates from a xenograft tumor arising from injection of PANC-1^{R15} cells in the flanks of athymic nude mice treated with (+) or without (-) DOX were also examined.

To confirm if KRAS inhibition alters SFRP2 expression, we inhibited KRAS activity by a second method using a KRAS^{G12D} inhibitor, MRTX1133 (Selleckchem, E1051, Houston, TX) [31], on PANC-1 pancreatic cancer cells and performing western blot prob-

ing for SFRP2. In this experiment, PANC-1 cells were treated with MRTX1133 (20 μM from 4 to 48 hours, or 10 μM for 24 and 48 hours). Negative controls included media alone for the initial time point and 20 nM DMSO (#D2650) for the 48-hour time point (Sigma, St. Louis, MO, USA). When the 4-hour timepoint required to visualize the maximum effects of KRAS inhibition on SFRP2 expression was established, a second cell line, MIA PaCa-2, was tested to confirm the involvement of KRAS signaling through the RAF/MEK and PI3K pathway in SFRP2 regulation. Cells were treated with the B-RAF inhibitor, dabrafenib, at 0.1 μM (Selleckchem, 1195768-06-9), the MEK inhibitor, trametinib, at 100 nM (Selleckchem, 1187431-43-1), or the PI3K inhibitor, buparlisib, at 1 uM (Selleckchem, 944396-07-0) for 4 hours. Cells were then lysed and probed for Phospho-ERK, ERK, and SFRP2 using western blot analysis.

2.10. Western blot analysis

The protein content was equalized across samples using a Bradford solution, Bio-Rad Protein Assay (#500-0205, Bio-Rad Laboratories). Samples containing equal amounts of total protein were run on 10% bis-tris SDS-PAGE gels (#NW00100BOX Invitrogen) for 1 hour at 140 V. Proteins were transferred onto a PVDF membrane (#LC2005 Life Technologies; Carlsbad, CA, USA) at 30 V for 70 min. Membranes were then incubated for 30 min at RT in blocking buffer (PBS, Twin 0.1%, 5% milk), and then at 4°C overnight with the primary antibody resuspended in blocking buffer. The following day, membranes were incubated with a HRP-conjugated secondary antibody (1:5000) for 1 hour at RT. The ECL Prime Western Blotting System was used to visualize protein bands (#RPN2232; GE Healthcare). Protein levels from test samples were compared to the loading controls (actin, GAPDH, or vinculin). To do this, densities were calculated by multiplying the average intensity by the surface of each band, and the percentage of control was calculated using the following formula: marker of interest total density x 100/loading control total density. For each experimental sample, values were then normalized to a control which was given the value of 1.00.

2.11. Statistical analysis

Paired t-test was used to compare the protein levels of SFRP2 between pancreatic tumor samples and SFRP2 protein levels in matched, normal adjacent tis-

sue. Calculation of Spearman correlation coefficient was conducted by using the Spearman correlation coefficient equation $\rho = 1 - (6\Sigma d_i^2)/(n(n^2 - 1))$ after ranking the level of SFRP2 mRNA expression and the ESTIMATE stromal expression, and after ranking the level of SFRP2 immunohistochemical staining and fibrosis level by Masson trichome and picrosirius red staining. Statistical analyses were performed using Stata (version v16.1, College Station, TX, USA). P-values of < 0.05 were considered statistically significant.

3. Results

3.1. SFRP2 RNA levels are the highest in pancreatic cancer and are associated with poor survival

SFRP2 protein is present in multiple cancers including angiosarcoma, hepatocellular carcinoma, prostate, colon, renal, lung, ovarian, and pancreatic cancers [7]. Therefore, we first assessed which cancer had the highest SFRP2 expression levels. To evaluate *SFRP2* mRNA levels, we used the RNAseq data from the TCGA. We collected RNAseq data for *SFRP2* expression from all 32 cancer types in the database (Fig. 1A). The median number of samples for each cancer type was 294 (range 36-1,082). Pancreatic cancer was found to have the highest levels of *SFRP2* mRNA compared to all other tumor types, with a median expression of 13,155 RNAseq by expectation maximization (RSEM) (5.11-120,416 RSEM). In the vast majority of tumor samples among the 32 types of cancer, the *SFRP2* gene was not mutated. Next, we compared the mRNA expression levels between normal pancreas and pancreatic adenocarcinoma using the GEPIA online tool. Pancreatic adenocarcinoma mRNA expression data were obtained from the TCGA RNAseq database ($n = 179$), and normal pancreas mRNA expression data were from the GTex RNAseq database ($n = 177$). *SFRP2* mRNA levels in pancreatic adenocarcinoma were significantly higher than in normal pancreas ($p < 0.01$; Fig. 1B).

The GEPIA online tool was used to evaluate the association between *SFRP2* mRNA expression and disease-free survival for pancreatic cancer patients. High *SFRP2* mRNA levels were defined as *SFRP2* mRNA expression in the 50th percentile or higher, and low *SFRP2* mRNA levels were defined as *SFRP2* mRNA expression in the 20th percentile or lower. Disease-free survival was compared between high *SFRP2* mRNA levels ($n = 89$) and low *SFRP2* mRNA levels ($n = 36$) using the Kaplan-Meier method. High *SFRP2* mRNA levels were associated with significantly decreased disease-free survival (hazard ratio = 2.6; $p = 0.0097$; Fig. 1C).
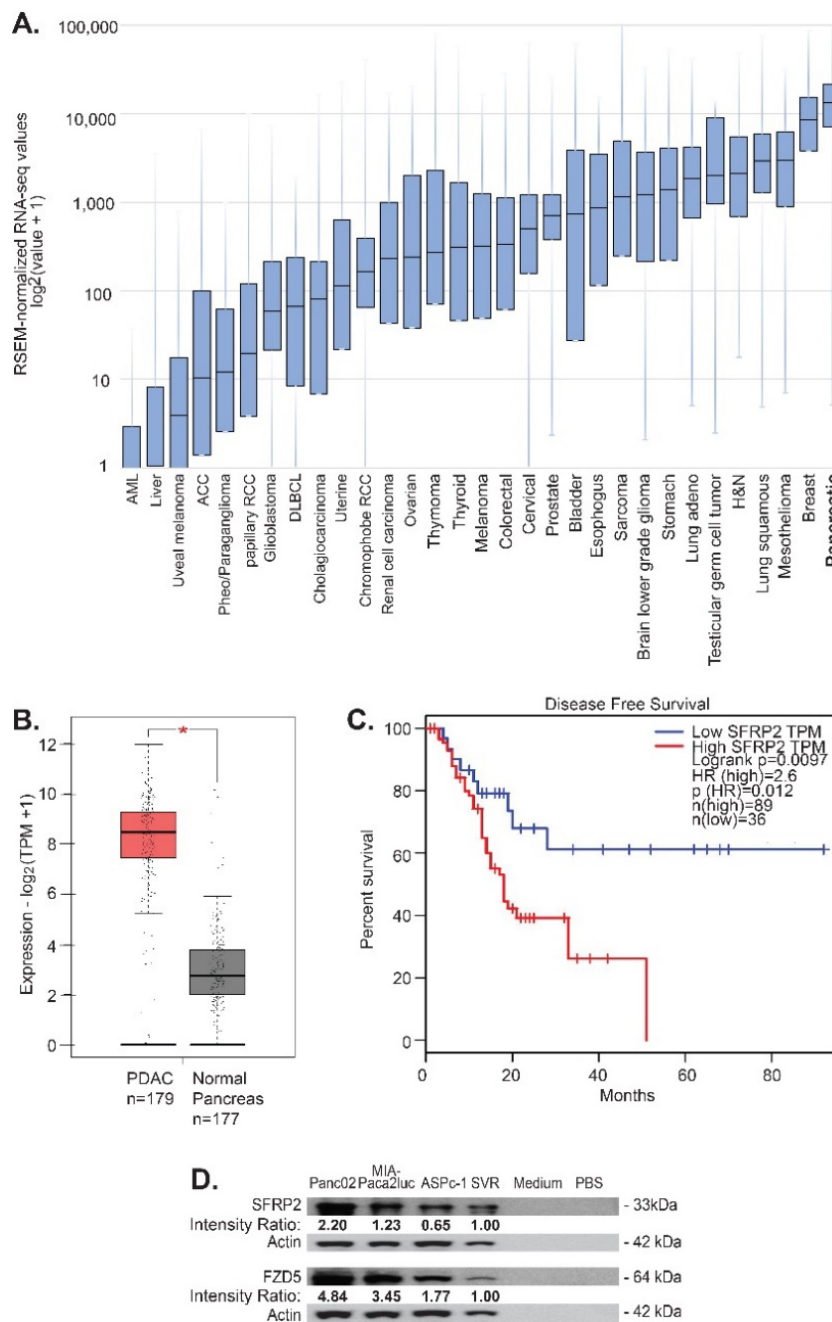
Fig. 1. *SFRP2* mRNA expression is increased in pancreatic cancer. (A) *SFRP2* mRNA levels were compared between 32 cancer types in the TCGA database. Pancreatic cancer had the highest *SFRP2* median expression levels. (B) The online interactive tool GEPIA was used to compare *SFRP2* mRNA levels between pancreatic cancer samples ($n = 179$) from the RNAseq TCGA database, and normal pancreas samples ($n = 177$) from the RNAseq GTex database. *SFRP2* mRNA levels were significantly higher in pancreatic adenocarcinoma samples, compared to normal pancreas samples (*$p < 0.01$). (C) GEPIA was used to compare disease-free survival between patients with high SFRP2 mRNA levels ($n = 89$), and low *SFRP2* RNA levels ($n = 36$) using the Kaplan-Meier method. High *SFRP2* expression was associated with significantly worse disease-free survival (hazard ratio = 2.6; $p = 0.0097$). HR: Hazard ratio. (D)SFRP2 and FZD5 protein levels were measured by western blot on lysates from pancreatic cancer cell lines (AsPC-1, MIA-PaCa2, and Panc02-luc) and compared to a known positive control, SVR (angiosarcoma cells), and negative controls (PBS and media). Band densities (average intensity x band surface) were normalized to the loading control to eliminate inter-sample variability to obtain the Intensity Ration. Results were normalized to the positive control, SVR.
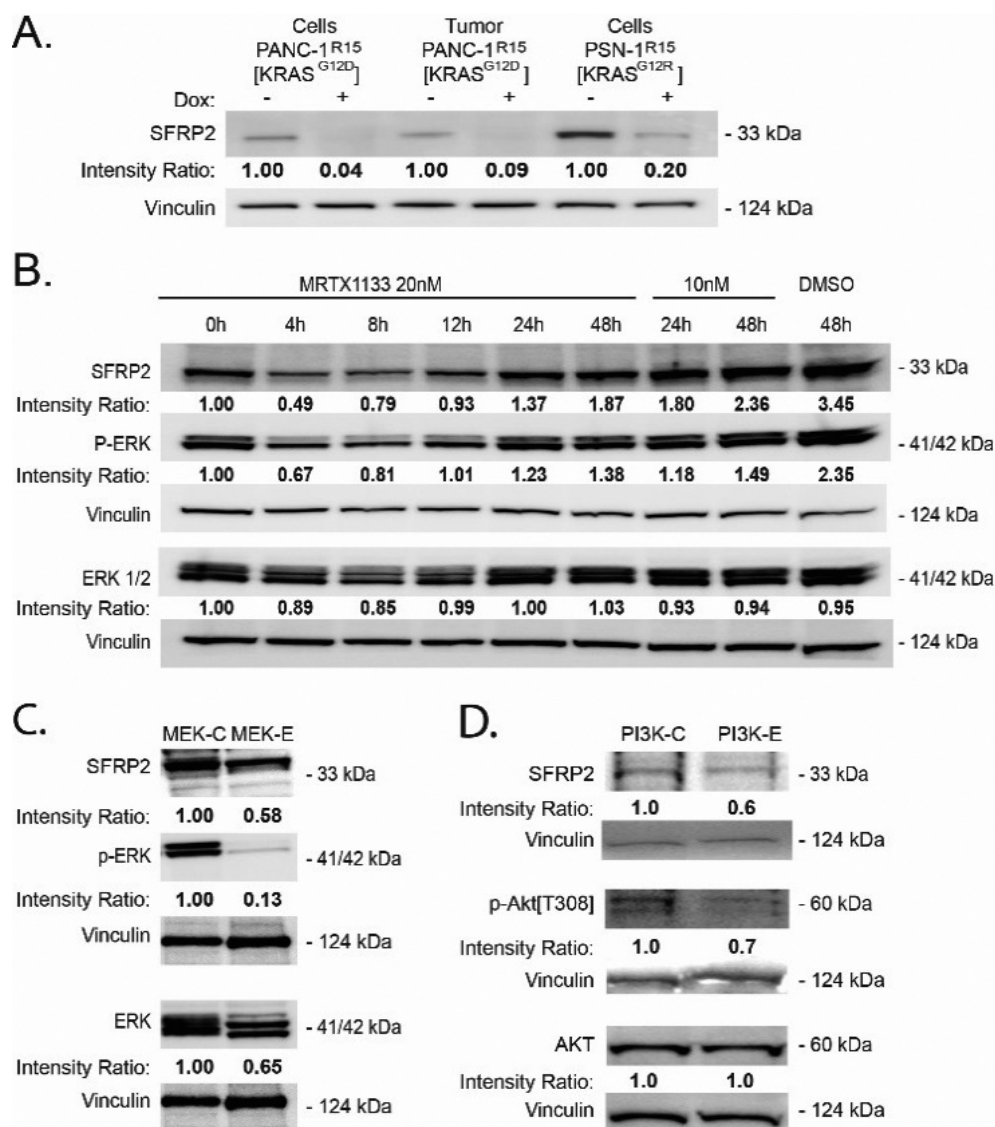
Fig. 2. Inhibition of KRAS reduces SFRP2 expression in PDAC. A, B, C, D) Band densities (average intensity x band surface) were normalized to the loading control, Vinculin, to eliminate inter-sample variability, to quantitatively obtain the Intensity Ratio. For each cell type, results were normalized to the untreated control: -Dox (A), and 0 h (B). (A) Western blot analysis of PDAC expressing a doxycycline (DOX)-inducible CFP-R15 monobody. DOX-induced R15 (+) reduced SRFP2 levels in both PDAC lines and a PANC-1 tumor sample. DOX: doxycycline. (B) Western blot analysis of PANC-1 cells treated with DMSO or MRTX1133 (10 or 20 nM), a noncovalent selective KRAS^{G12D} inhibitor, for various periods of time shows a reduction of p-ERK and SFRP2 at 4 hours compared to control. (C) Treatment of MIA PaCa-2 cells with trametinib (MEK inhibitor) at 100 nm for 4 hours shows a reduction in p-ERK and SFRP2. (D) Treatment of MIA PaCa-2 cells with buparlisib (PI3Kinase inhibitor) at 1 uM for 4 hours shows a reduction in p-AKT and SFRP2 compared to control.

3.2. SFRP2 protein and its receptor, FZD5, are expressed in pancreatic cancer cell lines in vitro

We previously showed that frizzled-5 (FZD5) is the receptor for SFRP2 in the non-canonical WNT-calcineurin pathway in endothelial, angiosarcoma, and breast cancer cells [25]. Therefore, we measured SFRP2 and FZD5 protein levels in pancreatic cell lines. Both

KRAS and *p53* mutation-bearing cell lines were selected, since they are the most common mutations in pancreatic cancer, with a rate of 90% and 75%, respectively for each marker [32]. SFRP2 and FZD5 protein levels were assessed by western blot in two human pancreatic cancer cell lines, AsPC-1 and MIA-PaCa2, and one murine cell line, Panc02-luc. SFRP2 and FZD5 protein levels were further compared to the levels in SVR

angiosarcoma, used as a positive control [25]. PBS and media were used as negative controls. All three pancreatic cell lines showed high SFRP2 and FZD5 protein levels compared to the positive control, with no protein in the negative controls (Fig. 1D).

3.3. KRAS regulates SFRP2 protein in PDAC cells

To determine whether mutant KRAS influences SRFP2 expression, we utilized the recently described R15 monobody to directly inhibit oncogenic RAS activity in PDAC cells (Fig. 2A) [21]. DOX-induced expression of R15 in either PANC-1^{R15} or PSN-1^{R15} led to a reduction in SRFP2 protein levels. In addition, PANC-1^{R15} xenograft tumors treated with the monobody contained lower SFRP2 levels than untreated tumors (Fig. 2A), further supporting regulation of SFRP2 expression by mutant KRAS signaling in PDAC. To confirm this result with a different KRAS inhibitor, PANC-1 cells were treated with MRTX1133, a noncovalent and selective inhibitor of KRAS^{G12D}, for periods of time ranging from 0 to 48 hours. As shown in Fig. 2B, MRTX1133 reversibly inhibited the activity of ERK, a known target of KRAS^{G12D}, and reduced the expression SFRP2, with a maximum effect at 4 hours. To further evaluate downstream mediators of the KRAS pathway, MIA PaCa-2 cells were treated with dabrafenib (B-Raf inhibitor) and trametinib (MEK inhibitor), which reduced phospho-ERK and SFRP2 protein levels (Fig. 2C). Likewise, the inhibition of PI3Kinase by buparlisib, another downstream target of KRAS, reduced phospho-AKT and SFRP2 protein levels (Fig. 2D). This demonstrates that in pancreatic cancer, SFRP2 is regulated by both KRAS/RAF/MEK/ERK and KRAS/ PI3Kinase pathways.

3.4. SFRP2 protein expression is increased in human pancreatic cancer compared to adjacent normal pancreatic tissue

To compare SFRP2 protein expression levels in human pancreatic cancer to matched normal adjacent pancreatic tissue, we measured the levels of SFRP2 protein by western blot in 23 pairs of samples. Table 1 shows the clinical characteristics of these patients. Forty-two percent were male, and the median age was 67.5 (range 47–87). Seventy five percent of the patients were Caucasian while the remaining 25% were non-Hispanic Blacks. Seventy-five percent of patients had Stage IIB disease (ranged from IA to IIB). The densitometry

Table 1
Clinical Characteristics of Patients Analyzed

Clinical factors	$n = 24$
Age, median (range)	65 (47–87)
Sex (N%)	
Female	14 (58.3)
Male	10 (41.7)
Race (N%)	
Black	6 (25.0)
White	18 (75.0)
Tumor Grade (N%)	
Well differentiated	1 (4.2)
Moderately differentiated	16 (66.7)
Poorly differentiated	5 (20.8)
Missing	2 (8.3)
Stage (N%)	
IA-IIA	6 (25.0)
IIB	18 (75.0)
Last Follow-up, median (range)	21 months (4–92 months)

of SFRP2 protein bands was measured in tumor and normal tissues and normalized to the loading control, GAPDH, for each tumor and matched normal tissue assessed. Results showed significantly higher expression of SFRP2 in tumor tissues with an average percent GAPDH of $57.0 \pm 5.69\%$ compared to $27.8 \pm 7.86\%$ in the normal adjacent tissue ($p = 0.0003$; $n = 23$; one patient sample was excluded from the analysis due to poor quality of the sample; Fig. 3A–B and Supplemental Fig. 1).

3.5. SFRP2 expression is associated with fibrosis in pancreatic cancer

Pancreatic cancer has the highest stroma content of any solid organ tumor, which is a major barrier to chemotherapy tumor biodistribution [6]. Since SFRP2 is associated with fibrosis in other pathologies [18], including cancers [19], we hypothesized that SFRP2 expression levels would be associated with the degree of fibrosis in pancreatic cancer. *SFRP2* mRNA expression from pancreatic cancer patients in the TCGA ($n = 176$, consisting of 95 men, 80 women, and 1 unknown) was correlated with the ESTIMATE stromal score [30], and the Spearman correlation coefficient between *SFRP2* mRNA expression levels and stromal score was 0.81 (Fig. 4).

Next, we tested the correlation between fibrosis in pancreatic tumors and SFRP2 protein expression in tumors in vivo. KPC mice ($n = 8$) developed PDAC about 4–5 months after Cre-recombinase induction with tamoxifen. After autopsy (average 153 days after induction with tamoxifen, range 116–203 days), pancreatic tumors were resected and paraffin-embedded for staining. Masson trichome staining and picrosirius red
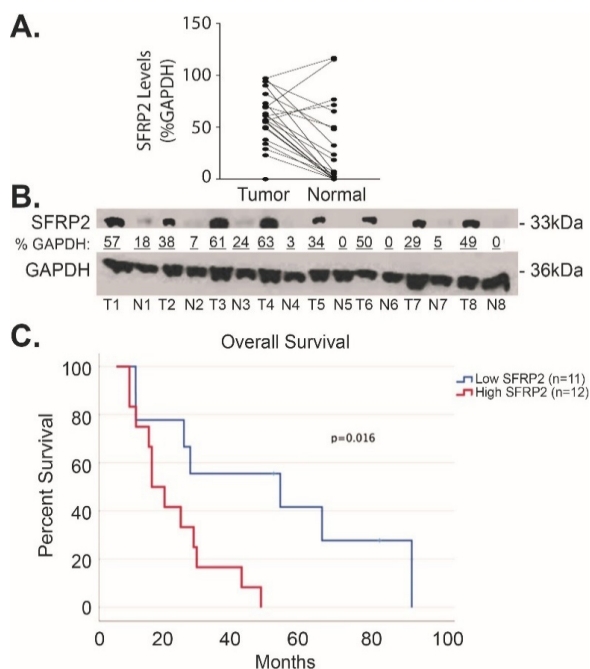
Fig. 3. SFRP2 protein expression is increased in pancreatic cancer. (A) Blot plot of the densitometry values from representative western blot comparing the levels of SFRP2 between tumor tissue from patients in Table 1 and their normal adjacent pancreatic tissue. (B) Representative western blot of tumor tissues (T) and their normal adjacent tissues (N). Densitometry was calculated by measuring the total intensity of each SFRP2 band in tumor and normal samples, and comparing them to the loading control, GAPDH.
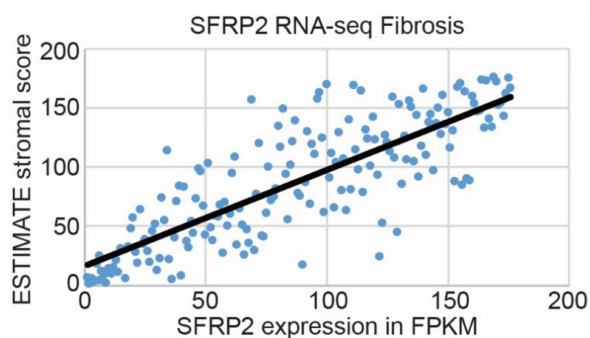

Fig. 4. SFRP2 RNA expression is associated with fibrosis in pancreatic cancer. mRNA expression of SFRP2 in pancreatic cancer patient samples from the TCGA ($n = 176$, consisting of 95 men, 80 women, and 1 unknown) correlates with the ESTIMATE stromal score obtained from RNAseq data on those patients. Spearman correlation coefficient is 0.81.

were used to determine the degree of fibrosis in the tumors. SFRP2 staining was also performed in consecutive sections. Tumors were ranked by their degree of fibrosis, and SFRP2 staining was ranked by intensity level. Fibrosis was associated with SFRP2 staining

with a Spearman correlation coefficient of 0.75 (Fig. 5). Taken together, our analysis of human pancreatic cancer datasets and tumors from genetically engineered mouse models demonstrate a strong correlation between SFRP2 expression and the degree of stromal expansion in pancreatic tumors.

3.6. SFRP2 promotes the mesenchymal transformation of fibroblasts

Because we consistently observed a positive correlation between SFRP2 levels and fibrosis, and since SFRP2 is connected to epithelial-mesenchymal transition (EMT) in network analysis [18], we hypothesized that SFRP2 induces a mesenchymal transformation in fibroblasts. To test this hypothesis, we used two cell types: normal human skin fibroblasts and normal mouse pancreatic fibroblasts. Cells were treated for 48 hours either with TFGβ (5 nM; positive control), or with SFRP2 (30 nM), or were not treated (negative control). Whole cell lysates were screened for N-cadherin and fibronectin protein expression by western blot. The protein levels of the first mesenchymal marker tested, N-cadherin, were approximately 2-fold higher in TGFβ- and SFRP2-treated skin fibroblasts compared to untreated control. A similar result was obtained for mouse pancreatic fibroblasts with a 2-fold increase in N-cadherin protein levels with TFGβ treatment, and a 3-fold increase with SFRP2 treatment (Fig. 6A). The protein levels of the second mesenchymal marker tested, fibronectin, were increased by 2-fold and 5-fold in TGFβ- and SFRP2-treated human fibroblasts, respectively (Fig. 6B). Although not as robust, we observed an increase in fibronectin protein levels with both TGFβ (80%) and SFRP2 (50%) in mouse pancreatic fibroblasts. These results demonstrate that like TGFβ, a well-known EMT inducer, SFRP2 plays a role in the EMT process, at least by inducing the upregulation of mesenchymal markers.

4. Discussion

The challenges surrounding pancreatic cancer treatment lie in its tremendous resistance to chemotherapeutics. The dense stroma of pancreatic cancer is a key contributor to this resistance, establishing an environment with low vascularity that impedes drug delivery and immune cell infiltration [4]. In this study, we found SFRP2 to be highly expressed in pancreatic cancer compared to normal adjacent pancreatic tissue, and high *SFRP2* ex-
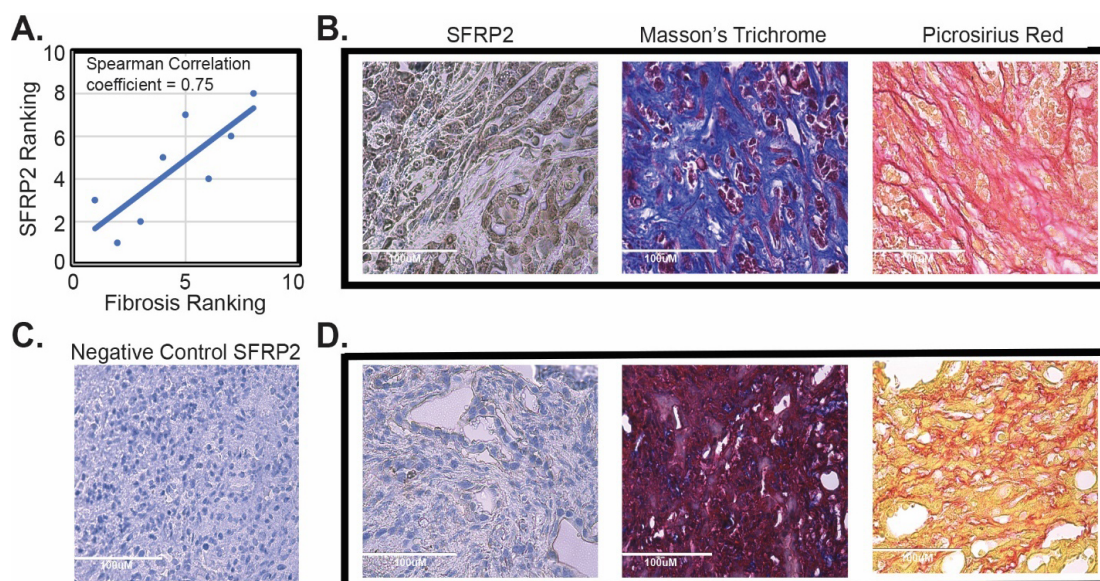
Fig. 5. SFRP2 expression is associated with fibrosis *in vivo*. (A) Correlation of SFRP2 staining and degree of fibrosis in tumors from KPC mice ($n = 8$). (B) Representative images of staining from a KPC mouse that had high SFRP2 staining and high levels of fibrosis identified by Masson's trichome blue staining and picrosirius red staining. (C) Negative control for SFRP2 immunohistochemistry staining. (D) Representative images of staining from a KPC mouse that had low SFRP2 staining and low levels of fibrosis identified by Masson's trichome purple staining and picrosirius yellow staining. All slides at 40X HPF: High Power Field. Scale bar: 100 μm.
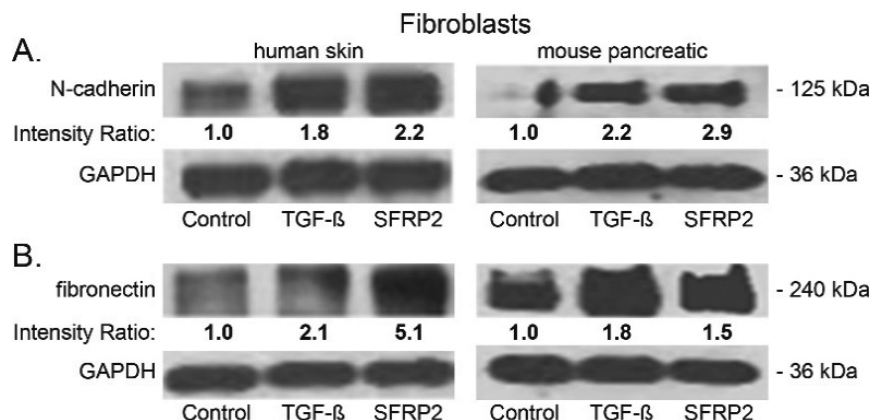

Fig. 6. SFRP2 induces epithelial mesenchymal transformation and collagen production in fibroblasts. (A) Human skin and mouse pancreatic fibroblasts were either untreated (control) or treated for 48 hours with SFRP2 (30 nM) or TGFβ (5 nM), and protein levels were analyzed by western blot. Band densities (average intensity x band surface) were normalized to the loading control, GAPDH, to eliminate inter-sample variability. Results were normalized to the untreated control and presented as intensity ratio. (A, B) TGFβ and SFRP2 treatments induce an increase of N-cadherin (A) and fibronectin (B) protein levels in both human skin and mouse pancreatic fibroblasts.

pression was predictive of worse survival using a TCGA data set. Based on these findings, a future prospective clinical study to confirm the high and low cutoffs will need to be obtained in future prospective clinical trials. SFRP2 as a reliable biomarker is warranted. SFRP2 also correlated with pancreatic cancer fibrosis, and fibroblasts treated with SFRP2 protein expressed higher levels of mesenchymal markers involved in EMT, a phenotype

that correlates with cancer invasion and metastasis.

With the TCGA RNAseq data, we found that SFRP2 expression levels are the highest in pancreatic cancer. Conversely, both SFRP2 mRNA and protein levels appeared to be significantly lower in normal pancreatic tissue, compared to adjacent tumor tissue. This suggests that the neoplastic transformation of the pancreatic tissue correlates with an upregulation of SFRP2. *KRAS*

mutation is the most frequent mutation in PDAC, occurring in more than 90% of tumors [2], and our data show that SFRP2 protein levels in PDAC are regulated by KRAS activity. SFRP2 has the potential to serve as a prognostic biomarker and is a potential therapeutic target, which both warrant further investigation.

In this study we found that fibroblasts treated with SFRP2 had increase protein levels of N-cadherin and fibronectin, similar to TGFβ. Both N-cadherin and fibronectin are well-known mesenchymal markers involved in migration and invasion during tumor progression [6]. TGFβ is one of the strongest promoters of EMT, and it upregulates N-cadherin, leading to E-cadherin/N-cadherin ratio switching from E-cadherin being the dominant cadherin expressed in epithelial cells to N-cadherin being mainly expressed in mesenchymal cells [33]. Upregulation of N-cadherin plays a larger role in cancer metastasis compared to loss of E-cadherin [34,35] . Our observation that SFRP2 and TGFβ have similar effects on fibroblasts suggests that SFRP2 affects the mesenchymal status of the cells. A previous study on wound healing demonstrated that fibroblasts are predominant in the wound during the proliferation stage [36]. Importantly, this study showed that fibroblasts have the highest gene expression of EMT markers while concomitantly, SFRP2 is one of the most upregulated plasma membrane proteins. In the setting of cancer, Guo and colleagues [37] demonstrated that SFRP2 promotes a mesenchymal phenotype in glioblastoma characterized by increased expression of mesenchymal genes in SFRP2-overexpressing cells, as well as increased SFRP2 in the mesenchymal-glioblastoma subtype. These results suggest a general function of SFRP2 as an EMT promoter during tumor progression in multiple cancers, a hypothesis that aligns with our previous observation that the inhibition of SFRP2 limits metastatic spread [15].

SFRP2 has been highly associated with fibrosis and EMT in other tumor types [19]. Sun and colleagues' investigation into cancer resistance after chemotherapy showed that SFRP2 was upregulated in CAFs subjected to cytotoxic therapy [38]. They also showed that WNT16B signaling is also enhanced , which further contributes to drug resistance. Inhibition of SFRP2 may dually affect chemoresistance by decreasing the tumor stroma, and decreasing the signaling that confers therapeutic resistance. There has been recent interest in targeting the stromal tissue for pancreatic cancer treatment to dismantle the barricade to chemotherapy and immune response. The results of therapeutics used for these effects have been contradictory thus far. A small molecule inhibitor of the sonic hedgehog pathway showed efficacy in preclinical studies [39] but failed to demonstrate improved survival in clinical trials [40,41]. Meanwhile, some improvements have been observed with other stromal inhibitors in phase I/II trials targeting TGFβ [42] and the angiotensin II receptor [43]. Conversely, Ozdemir and collaborators found that depleting myofibroblasts in a pancreatic cancer GEMM resulted in increased infiltration of regulatory T-cells and worse survival [44]. These results suggest that complete disruption of the tumor microenvironment may not bear the desired results of enhancing therapeutic efficacy.

Investigation of pancreatic CAFs has shown that this is a heterogeneous population of cells with different functions, which likely contributes to these different findings. Although Ozdemir and colleagues found that myofibroblast depletion led to more aggressive tumors and immune dysregulation, they also discovered that treating these myofibroblast-depleted mice with CTLA-4 checkpoint inhibitors led to less undifferentiated cancer cells, normalized parenchyma, and improved survival compared to non-myofibroblast depleted mice treated with anti-CTLA-4 antibody [44]. Therefore, inhibiting the stroma may need to be accompanied by immunotherapy for efficacy, and further studies will identify whether targeting the stroma overcomes resistance to immunotherapy in pancreatic cancer. We previously showed that SFRP2 affects immune dysregulation, specifically increasing transcription of CD38, which reduces resistance to the PD-1 inhibition [15]. Therefore, targeting SFRP2 may have the added benefit of providing immunotherapy, in conjunction with stromal regulation, inducing tumor apoptosis and inhibiting angiogenesis. Since SFRP2 is highly expressed in pancreatic cancer; its expression is significantly associated with worse survival, and it is regulated by KRAS; SFRP2 may serve as a novel therapeutic target for pancreatic cancer.

5. Conclusion

We demonstrated that SFRP2 is highly expressed in pancreatic cancer and its expression is significantly associated with worse disease-free survival and is regulated by KRAS. We confirmed that, like other cancer types, SFRP2 is associated with fibrosis in pancreatic cancer. Investigation of SFRP2's impact on fibroblasts showed that SFRP2 stimulates EMT, which identifies an additional role for SFRP2 as a regulator for cancer invasion, angiogenesis, metastasis, and ECM construc-

tion. Targeting the stroma is a promising avenue for pancreatic cancer treatment, but the current literature demonstrates that further research on the communication of all heterogeneous cell populations, cytokines, and proteins in the tumor microenvironment is needed to understand how best to manipulate it to improve survival. SFRP2 is one such protein that plays a part in this crosstalk and merits additional study to determine its potential as a regulator for both stroma production and immune dysregulation.

Acknowledgments

Author contributions

Conception: NKD, JBS, PN, JPO; Interpretation or analysis of data: JBS, PN, KLH, LS, RM, JPO, JEM, IK; LH, MG, BR, Preparation of the manuscript: JBS, PN, NKD, RM, IK, JPO, NGD, EH, LH; Revision for important intellectual content: NKD; Supervision: NKD, JBS, PN.

Supplementary data

The supplementary files are available to download from http://dx.doi.org/10.3233/CBM-220044.

References

[1]   R.L. Siegel, K.D. Miller, H.E. Fuchs and A. Jemal, Cancer Statistics, 2021, *CA Cancer J Clin* **71** (2021), 7–33.

[2]   B. Giri, V. Sethi, V. Dudeja and S. Banerjee, A. Livingstone and A. Saluja, Genetics of pancreatic cyst-cancer progression: standing on the shoulders of giants, *Curr Opin Gastroenterol* **33** (2017), 404–410.

[3]   E. Oneda and A. Zaniboni, Are We Sure that Adjuvant Chemotherapy is the Best Approach for Resectable Pancreatic Cancer? Are We in the Era of Neoadjuvant Treatment? A Review of Current Literature, *J Clin Med* **8** (2019).

[4]   D. Thomas and P. Radhakrishnan, Pancreatic Stellate Cells: The Key Orchestrator of The Pancreatic Tumor Microenvironment, *Adv Exp Med Biol* **1234** (2020), 57–70.

[5]   F. Polani, P.M. Grierson and K.H. Lim, Stroma-targeting strategies in pancreatic cancer: Past lessons, challenges and prospects, *World J Gastroenterol* **27** (2021), 2105–2121.

[6]   D. Thomas and P. Radhakrishnan, Tumor-stromal crosstalk in pancreatic cancer and tissue fibrosis, *Mol Cancer* **18** (2019), 14.

[7]   A. Courtwright, S. Siamakpour-Reihani, J.L. Arbiser, N. Banet, E. Hilliard, L. Fried, C. Livasy, D. Ketelsen, D.B. Nepal, C.M. Perou, C. Patterson and N. Klauber-DeMore, Secreted Frizzle-Related Protein 2 Stimulates Angiogenesis via a Calcineurin/NFAT Signaling Pathway, *Cancer Res* (2009).

[8]   M.E. Fane, B.L. Ecker, A. Kaur, G.E. Marino, G.M. Alicea, S.M. Douglass, Y. Chhabra, M.R. Webster, A. Marshall, R. Colling, O. Espinosa, N. Coupe, N. Maroo, L. Campo, M.R. Middleton, P. Corrie, X. Xu, G.C. Karakousis and A.T. Weeraratna, sFRP2 Supersedes VEGF as an Age-related Driver of Angiogenesis in Melanoma, Affecting Response to Anti-VEGF Therapy in Older Patients, *Clin Cancer Res* **26** (2020), 5709–5719.

[9]   A. Kaur, M.R. Webster, K. Marchbank, R. Behera, A. Ndoye, C.H. Kugel, 3rd, V.M. Dang, J. Appleton, M.P. O'Connell, P. Cheng, A.A. Valiga, R. Morissette, N.B. McDonnell, L. Ferrucci, A.V. Kossenkov, K. Meeth, H.Y. Tang, X. Yin, W.H. Wood, 3rd, E. Lehrmann, K.G. Becker, K.T. Flaherty, D.T. Frederick, J.A. Wargo, Z.A. Cooper, M.T. Tetzlaff, C. Hudgens, K.M. Aird, R. Zhang, X. Xu, Q. Liu, E. Bartlett, G. Karakousis, Z. Eroglu, R.S. Lo, M. Chan, A.M. Menzies, G.V. Long, D.B. Johnson, J. Sosman, B. Schilling, D. Schadendorf, D.W. Speicher, M. Bosenberg, A. Ribas and A.T. Weeraratna, sFRP in the aged microenvironment drives melanoma metastasis and therapy resistance, *Nature* **532** (2016), 250–4.

[10]   J.L. Lee, C.J. Chang, L.L. Chueh and C.T. Lin, Secreted Frizzled Related Protein 2 (sFRP2) Decreases Susceptibility to UV-Induced Apoptosis in Primary Culture of Canine Mammary Gland Tumors by NF-kappaB Activation or JNK Suppression, *Breast Cancer Res Treat* **100** (2006), 49–58.

[11]   M. Montagner, R. Bhome, S. Hooper, P. Chakravarty, X. Qin, J. Sufi, A. Bhargava, C.D.H. Ratcliffe, Y. Naito, A. Pocaterra, C.J. Tape and E. Sahai, Crosstalk with lung epithelial cells regulates Sfrp2-mediated latency in breast cancer dissemination, *Nat Cell Biol* **22** (2020), 289–296.

[12]   W. Roth, C. Wild-Bode, M. Platten, C. Grimmel, H.S. Melkonyan, J. Dichgans and M. Weller, Secreted Frizzled-related proteins inhibit motility and promote growth of human malignant glioma cells, *Oncogene* **19** (2000), 4210–4220.

[13]   P. Techavichit, Y. Gao, L. Kurenbekova, R. Shuck, L.A. Donehower and J.T. Yustein, Secreted Frizzled-Related Protein 2 (sFRP2) promotes osteosarcoma invasion and metastatic potential, *BMC Cancer* **16** (2016), 869.

[14]   S. Yamamura, K. Kawakami, H. Hirata, K. Ueno, S. Saini, S. Majid and R. Dahiya, Oncogenic functions of secreted Frizzled-related protein 2 in human renal cancer, *Mol.Cancer*

Ther. **9** (2010), 1680–1687.

[15] P. Nasarre, D.I. Garcia, J.B. Siegel, I.V. Bonilla, R. Mukherjee, E. Hilliard, P. Chakraborty, C. Nasarre, J.T. Yustein, M. Lang, A.A. Jaffa, S. Mehrotra and N. Klauber-DeMore, Overcoming PD-1 Inhibitor Resistance with a Monoclonal Antibody to Secreted Frizzled-Related Protein 2 in Metastatic Osteosarcoma, *Cancers (Basel)* **13** (2021).

[16] D. Garcia, P. Nasarre, I.V. Bonilla, E. Hilliard, Y.K. Peterson, L. Spruill, A.M. Broome, E.G. Hill, J.T. Yustein, S. Mehrotra and N. Klauber-DeMore, Development of a Novel Humanized Monoclonal Antibody to Secreted Frizzled-Related Protein-2 That Inhibits Triple-Negative Breast Cancer and Angiosarcoma Growth *In Vivo*, *Ann Surg Oncol* **26** (2019), 4782–4790.

[17] K. Kobayashi, M. Luo, Y. Zhang, D.C. Wilkes, G. Ge, T. Grieskamp, C. Yamada, T.C. Liu, G. Huang, C.T. Basson, A. Kispert, D.S. Greenspan and T.N. Sato, Secreted Frizzled-related protein 2 is a procollagen C proteinase enhancer with a role in fibrosis associated with myocardial infarction, *Nat Cell Biol* **11** (2009), 46–55.

[18] M. Mastri, Z. Shah, K. Hsieh, X. Wang, B. Wooldridge, S. Martin, G. Suzuki and T. Lee, Secreted Frizzled-related protein 2 as a target in antifibrotic therapeutic intervention, *Am J Physiol Cell Physiol* **306** (2014), C531–9.

[19] K.M. Vincent and L.M. Postovit, A pan-cancer analysis of secreted Frizzled-related proteins: re-examining their proposed tumour suppressive function, *Sci Rep* **7** (2017), 42719.

[20] E.C. Little, C. Wang, P.M. Watson, D.K. Watson, D.J. Cole and E.R. Camp, Novel immunocompetent murine models representing advanced local and metastatic pancreatic cancer, *J Surg Res* **176** (2012), 359–66.

[21] I. Khan, Koide, A., Zuberi, M., Ketavarapu, G., Denbaum, E., Teng, K.W., Rhett, M., Spencer-Smith, R., Hobbs, A.G., Camp, E.R., Koide, S., O'Bryan, J.P., Identification of the nucleotide-free state as a therapeutic vulnerability for inhibition of selected oncogenic RAS mutants, *Cell Reports* (2022).

[22] C.A. Feghali and T.M. Wright, Identification of multiple, differentially expressed messenger RNAs in dermal fibroblasts from patients with systemic sclerosis, *Arthritis Rheum* **42** (1999), 1451–7.

[23] J.L. Arbiser, M.A. Moses, C.A. Fernandez, N. Ghiso, Y. Cao, N. Klauber, D. Frank, M. Brownlee, E. Flynn, S. Parangi, H.R. Byers and J. Folkman, Oncogenic H-ras stimulates tumor angiogenesis by two distinct pathways., *Proc Natl Acad Sci USA* **94** (1997), 861–866.

[24] A. Gopinathan, J.P. Morton, D.I. Jodrell and O.J. Sansom, GEMMs as preclinical models for testing pancreatic cancer therapies, *Dis Model Mech* **8** (2015), 1185–200.

[25] Y.K. Peterson, P. Nasarre, I.V. Bonilla, E. Hilliard, J. Samples, T.A. Morinelli, E.G. Hill and N. Klauber-DeMore, Frizzled-5: a high affinity receptor for secreted frizzled-related protein-2 activation of nuclear factor of activated T-cells c3 signaling to promote angiogenesis, *Angiogenesis* **20** (2017), 615–628.

[26] E. Cerami, J. Gao, U. Dogrusoz, B.E. Gross, S.O. Sumer, B.A. Aksoy, A. Jacobsen, C.J. Byrne, M.L. Heuer, E. Larsson, Y. Antipin, B. Reva, A.P. Goldberg, C. Sander and N. Schultz, The cBio cancer genomics portal: an open platform for exploring multidimensional cancer genomics data, *Cancer Discov* **2** (2012), 401–4.

[27] J. Gao, B.A. Aksoy, U. Dogrusoz, G. Dresdner, B. Gross, S.O. Sumer, Y. Sun, A. Jacobsen, R. Sinha, E. Larsson, E. Cerami, C. Sander and N. Schultz, Integrative analysis of complex cancer genomics and clinical profiles using the cBioPortal, *Sci Signal* **6** (2013), pl1.

[28] Z. Tang, C. Li, B. Kang, G. Gao, C. Li and Z. Zhang, GEPIA: a web server for cancer and normal gene expression profiling and interactive analyses, *Nucleic Acids Res* **45** (2017), W98–W102.

[29] M. Uhlen, C. Zhang, S. Lee, E. Sjostedt, L. Fagerberg, G. Bidkhori, R. Benfeitas, M. Arif, Z. Liu, F. Edfors, K. Sanli, K. von Feilitzen, P. Oksvold, E. Lundberg, S. Hober, P. Nilsson, J. Mattsson, J.M. Schwenk, H. Brunnstrom, B. Glimelius, T. Sjoblom, P.H. Edqvist, D. Djureinovic, P. Micke, C. Lindskog, A. Mardinoglu and F. Ponten, A pathology atlas of the human cancer transcriptome, *Science* **357** (2017).

[30] in: *ESTIMATE: Estimation of STromal and Immune cells in MAlignant Tumor tissues using Expression data.*

[31] X. Wang, S. Allen, J.F. Blake, V. Bowcut, D.M. Briere, A. Calinisan, J.R. Dahlke, J.B. Fell, J.P. Fischer, R.J. Gunn, J. Hallin, J. Laguer, J.D. Lawson, J. Medwid, B. Newhouse, P. Nguyen, J.M. O'Leary, P. Olson, S. Pajk, L. Rahbaek, M. Rodriguez, C.R. Smith, T.P. Tang, N.C. Thomas, D. Vanderpool, G.P. Vigers, J.G. Christensen and M.A. Marx, Identification of MRTX1133, a Noncovalent, Potent, and Selective KRAS(G12D) Inhibitor, *J Med Chem* **65** (2022), 3123–3133.

[32] S.A. Sastra and K.P. Olive, Quantification of murine pancreatic tumors by high-resolution ultrasound, *Methods Mol Biol* **980** (2013), 249–66.

[33] Y. Ma, H. Zhang, C. Xiong, Z. Liu, Q. Xu, J. Feng, J. Zhang, Z. Wang and X. Yan, CD146 mediates an E-cadherin-to-N-cadherin switch during TGF-beta signaling-induced epithelial-mesenchymal transition, *Cancer Lett* **430** (2018), 201–214.

[34] S. Islam, T.E. Carey, G.T. Wolf, M.J. Wheelock and K.R. Johnson, Expression of N-cadherin by human squamous carcinoma cells induces a scattered fibroblastic phenotype with disrupted cell-cell adhesion, *J Cell Biol* **135** (1996), 1643–54.

[35] S. Nakajima, R. Doi, E. Toyoda, S. Tsuji, M. Wada, M. Koizumi, S.S. Tulachan, D. Ito, K. Kami, T. Mori, Y. Kawaguchi, K. Fujimoto, R. Hosotani and M. Imamura, N-cadherin expression and epithelial-mesenchymal transition in pancreatic carcinoma, *Clin Cancer Res* **10** (2004), 4125–33.

[36] F.Z. Gharbia, A.S. Abouhashem, Y.A. Moqidem, A.A. Elbaz, A. Abdellatif, K. Singh, C.K. Sen and H.M.E. Azzazy, Adult skin fibroblast state change in murine wound healing, *Sci Rep* **13** (2023), 886.

[37] M. Guo, K.M. Goudarzi, S. Abedi, M. Pieber, E. Sjoberg, J. Behnan, X.M. Zhang, R.A. Harris, J. Bartek, M.S. Lindstrom, M. Nister and D. Hagerstrand, SFRP2 induces a mesenchymal subtype transition by suppression of SOX2 in glioblastoma, *Oncogene* **40** (2021), 5066–5080.

[38] Y. Sun, D. Zhu, F. Chen, M. Qian, H. Wei, W. Chen and J. Xu, SFRP2 augments WNT16B signaling to promote therapeutic resistance in the damaged tumor microenvironment, *Oncogene* **35** (2016), 4321–34.

[39] K.P. Olive, M.A. Jacobetz, C.J. Davidson, A. Gopinathan, D. McIntyre, D. Honess, B. Madhu, M.A. Goldgraben, M.E. Caldwell, D. Allard, K.K. Frese, G. Denicola, C. Feig, C. Combs, S.P. Winter, H. Ireland-Zecchini, S. Reichelt, W.J. Howat, A. Chang, M. Dhara, L. Wang, F. Ruckert, R. Grutzmann, C. Pilarsky, K. Izeradjene, S.R. Hingorani, P. Huang, S.E. Davies, W. Plunkett, M. Egorin, R.H. Hruban, N. Whitebread, K. McGovern, J. Adams, C. Iacobuzio-Donahue, J. Griffiths and D.A. Tuveson, Inhibition of Hedgehog signaling enhances delivery of chemotherapy in a mouse model of pancreatic cancer, *Science* **324** (2009), 1457–61.

[40] A. De Jesus-Acosta, E.A. Sugar, P.J. O'Dwyer, R.K. Ramanathan, D.D. Von Hoff, Z. Rasheed, L. Zheng, A. Begum, R. Anders, A. Maitra, F. McAllister, N.V. Rajeshkumar, S. Yabuuchi, R.F. de Wilde, B. Batukbhai, I. Sahin and D.A.

Laheru, Phase 2 study of vismodegib, a hedgehog inhibitor, combined with gemcitabine and nab-paclitaxel in patients with untreated metastatic pancreatic adenocarcinoma, *Br J Cancer* **122** (2020), 498–505.

[41] A.H. Ko, N. LoConte, M.A. Tempero, E.J. Walker, R. Kate Kelley, S. Lewis, W.C. Chang, E. Kantoff, M.W. Vannier, D.V. Catenacci, A.P. Venook and H.L. Kindler, A Phase I Study of FOLFIRINOX Plus IPI-926, a Hedgehog Pathway Inhibitor, for Advanced Pancreatic Adenocarcinoma, *Pancreas* **45** (2016), 370–5.

[42] D. Melisi, R. Garcia-Carbonero, T. Macarulla, D. Pezet, G. Deplanque, M. Fuchs, J. Trojan, H. Oettle, M. Kozloff, A. Cleverly, C. Smith, S.T. Estrem, I. Gueorguieva, M.M.F. Lahn, A. Blunt, K.A. Benhadji and J. Tabernero, Galunisertib plus gemcitabine vs. gemcitabine for first-line treatment of patients with unresectable pancreatic cancer, *Br J Cancer* **119** (2018), 1208–1214.

[43] J.E. Murphy, J.Y. Wo, D.P. Ryan, J.W. Clark, W. Jiang, B.Y. Yeap, L.C. Drapek, L. Ly, C.V. Baglini, L.S. Blaszkowsky, C.R. Ferrone, A.R. Parikh, C.D. Weekes, R.D. Nipp, E.L. Kwak, J.N. Allen, R.B. Corcoran, D.T. Ting, J.E. Faris, A.X. Zhu, L. Goyal, D.L. Berger, M. Qadan, K.D. Lillemoe, N. Talele, R.K. Jain, T.F. DeLaney, D.G. Duda, Y. Boucher, C. Fernandez-Del Castillo and T.S. Hong, Total Neoadjuvant Therapy With FOLFIRINOX in Combination With Losartan Followed by Chemoradiotherapy for Locally Advanced Pancreatic Cancer: A Phase 2 Clinical Trial, *JAMA Oncol* **5** (2019), 1020–1027.

[44] B.C. Ozdemir, T. Pentcheva-Hoang, J.L. Carstens, X. Zheng, C.C. Wu, T.R. Simpson, H. Laklai, H. Sugimoto, C. Kahlert, S.V. Novitskiy, A. De Jesus-Acosta, P. Sharma, P. Heidari, U. Mahmood, L. Chin, H.L. Moses, V.M. Weaver, A. Maitra, J.P. Allison, V.S. LeBleu and R. Kalluri, Depletion of carcinoma-associated fibroblasts and fibrosis induces immunosuppression and accelerates pancreas cancer with reduced survival, *Cancer Cell* **25** (2014), 719–34.